Atmos. Chem. Phys., 10, 5999–6006, 2010
www.atmos-chem-phys.net/10/5999/2010/
doi:10.5194/acp-10-5999-2010

Atmospheric Chemistry and Physics

Geoengineering by stratospheric SO_2 injection: results from the Met Office HadGEM2 climate model and comparison with the Goddard Institute for Space Studies ModelE

A. Jones[1], **J. Haywood**[1], **O. Boucher**[1], **B. Kravitz**[2], **and A. Robock**[2]

[1]Met Office Hadley Centre, Exeter, UK
[2]Department of Environmental Sciences, Rutgers University, New Brunswick, NJ, USA

Received: 25 February 2010 – Published in Atmos. Chem. Phys. Discuss.: 22 March 2010
Revised: 16 June 2010 – Accepted: 17 June 2010 – Published: 5 July 2010

Abstract. We examine the response of the Met Office Hadley Centre's HadGEM2-AO climate model to simulated geoengineering by continuous injection of SO_2 into the lower stratosphere, and compare the results with those from the Goddard Institute for Space Studies ModelE. Despite the differences between the models, we find a broadly similar geographic distribution of the response to geoengineering in both models in terms of near-surface air temperature and mean June–August precipitation. The simulations also suggest that significant changes in regional climate would be experienced even if geoengineering was successful in maintaining global-mean temperature near current values, and both models indicate rapid warming if geoengineering is not sustained.

1 Introduction

Over the last decade, global warming has been well documented in both observational records and in simulations with climate models (IPCC, 2001, 2007). Furthermore, scenarios of unmitigated ("business as usual") future climate with these models suggest an increasingly rapid global-mean warming over the next century. The primary cause of global warming is from increased atmospheric concentrations of greenhouse gases (GHG) such as carbon dioxide, methane and nitrous oxide, as a result of anthropogenic activity. These gases exert a positive radiative forcing of climate and hence induce a warming. Increases in concentrations of aerosols are thought to ameliorate the effects of global warming via their impacts on radiation (direct effects) and on clouds (indirect effects), whereby they exert a negative radiative forcing of climate and hence induce a cooling (e.g., Haywood and Schulz, 2007). Recently, utilizing these cooling effects from aerosols has been suggested as emergency geoengineering measures to counterbalance the effects of global warming.

The impact of brightening stratocumulus clouds via injection of cloud condensation nuclei into low-level stratocumulus clouds has been investigated by Jones et al. (2009) using one of the models used in the present study. They suggest that, although the global-mean warming from increased GHG concentrations can indeed be reduced, there are significant geographical changes in temperature and precipitation patterns which could have adverse effects on some regions of the Earth such as Amazonia. The impact of the injection of sulphur dioxide (SO_2) into the stratosphere has also received much attention, formerly through the eruption of volcanoes with large stratospheric sulphate injections (e.g., Robock, 2000) and latterly through deliberate geoengineering (e.g., Rasch et al., 2008; Robock et al., 2008). Once again, the potential non-uniformity of the response to the geoengineering is highlighted. Here we examine the response of two climate models to geoengineering by injection of SO_2 into the lower stratosphere. The two models used are the Met Office Hadley Centre's HadGEM2-AO and the National Aeronautics and Space Administration Goddard Institute for Space Studies ModelE.

HadGEM2-AO is the fully-coupled atmosphere-ocean version of the Hadley Centre Global Environment Model version 2 (Collins et al., 2008). The atmosphere has a horizontal resolution of 1.25° latitude by 1.875° longitude, with 38 vertical levels up to about 40 km. This is coupled to a 40-level ocean/sea-ice model with a zonal resolution of 1° and

Correspondence to: A. Jones
(andy.jones@metoffice.gov.uk)

meridional resolution of 1° from the poles to 30°, thereafter varying smoothly to 1/3° at the equator. The sulphate aerosol scheme is described in Jones et al. (2001) and Bellouin et al. (2007). Briefly, the scheme includes gaseous and aqueous phase reactions of SO_2 to sulphuric acid and sulphate aerosol, with partitioning between Aitken, accumulation and dissolved modes and parameterisations for inter-modal transfers. The optically-active accumulation mode has a median radius of 0.095 µm and geometric standard deviation of 1.4, with hygroscopic growth based on d'Almeida et al. (1991). In the stratosphere the gaseous phase oxidation pathway of SO_2 to H_2SO_4 via reactions with the hydroxyl radical dominates, with concentrations of the hydroxyl radical being prescribed. An additional parameterisation for aerosol gravitational sedimentation was added to the scheme as this process is important for stratosphere/troposphere aerosol transport.

ModelE is also a coupled atmosphere-ocean model. The stratospheric version of the model was used (Schmidt et al., 2006), which has a horizontal resolution of 4° latitude by 5° longitude with 23 vertical levels up to 80 km. This is coupled to a 13 level ocean model with the same horizontal resolution (Russell et al., 1995). The sulphate aerosol scheme of ModelE is described in Koch et al. (2006). The model forms sulphate aerosols from SO_2 by reaction with the hydroxyl radical, which is prescribed. The dry aerosol effective radius is specified to be 0.25 µm with growth in response to ambient humidity following Tang (1996), resulting in a gamma distribution with an effective radius of 0.30–0.35 µm.

Both models include wet and dry aerosol deposition (Bellouin et al., 2007, and Koch et al., 2006, for HadGEM2 and ModelE, respectively), and the aerosol radiative forcing in both models is fully interactive with the atmospheric circulation.

2 Experimental design

The experimental designs were somewhat different for the two models, but are sufficiently similar for a comparison to be useful. The ModelE simulations are a subset of those reported in Robock et al. (2008). They comprise (i) a 3-member ensemble following the IPCC A1B scenario (Nakićenović et al., 2000) run for 40 years from 1999; (ii) another 3-member A1B ensemble plus geoengineering by SO_2 injection at a point over [0° N, 120° E] into the tropical lower stratosphere (ca. 16–23 km altitude) at a constant rate of $5\,\mathrm{Tg[SO_2]\,yr^{-1}}$ for the first 20 years, after which geoengineering is terminated and the simulation continued for a further 20 years; and (iii) a 2-member Control ensemble run in perpetual 1999 conditions for 40 years. As the variability between members is small (Robock et al., 2008) only the ensemble means are used. The presentation of results from ModelE follows that in Robock et al. (2008) in showing the difference from the perpetual 1999 Control simulation, to minimise the effect of any climate drift.

Three HadGEM2 simulations were performed, following on from a 20th century simulation using historical forcings: A1B and A1B-plus-geoengineering simulations, each of 60 years duration, and also a third simulation where SO_2 injection was suspended after 25 years. Given the lower vertical extent of the atmosphere component of HadGEM2 compared with ModelE (40 vs. 80 km), which has implications for the simulation of stratospheric dynamics, a more idealized approach was taken to simulating the geoengineering. A globally uniform injection of SO_2 into the lower stratosphere was used, at altitudes similar to those in the ModelE simulations and at the same rate of $5\,\mathrm{Tg[SO_2]\,yr^{-1}}$. The fact that poleward transport of stratospheric aerosol in ModelE is a little too fast (Robock et al., 2008) furthers the general similarity of the two approaches. Tests show that, for the constant SO_2 injection rate applied here, the stratospheric aerosol burden stabilises after 3–4 years.

As the ModelE simulations only included SO_2 injection for the first 20 years, the comparison will generally focus on the mean difference between the A1B-plus-geoengineering and A1B simulations over the second decade (years 11–20 inclusive) for each model.

3 Results

3.1 Sulphate aerosol

Figure 1 shows the burden of sulphate aerosol from geoengineering in the two models, calculated as the difference between the A1B and A1B-plus-geoengineering simulations, meaned over years 11–20. The corresponding aerosol optical depths are 0.050±0.001 and 0.090±0.004 for HadGEM2 and ModelE, respectively (decadal means±one standard deviation, at a wavelength of 550 nm). The global mean burden in HadGEM2 is about 70% of that in ModelE, resulting from the numerous differences in model formulation. However, both show a similar geographic distribution of geoengineering aerosol, with higher values at higher latitudes due to poleward transport by the large-scale circulation. Burdens are higher over the Arctic than the Antarctic in both models due to the stronger wave-driven stratospheric meridional circulation in the Northern Hemisphere (e.g., Rosenlof, 1995). The difference in relative sulphate burden over Antarctica is thought to be related to the models' simulation of the Antarctic polar vortex. This acts as a barrier to aerosol transport from lower latitudes, and the simulation of the vortex may be affected by the difference in resolution of the two models. The small equatorial maximum in the ModelE distribution is due to the point-injection on the equator used in that model. The general similarity in the distribution of the geoengineered aerosol in the two models indicates that the different SO_2 injection strategies employed makes little difference.

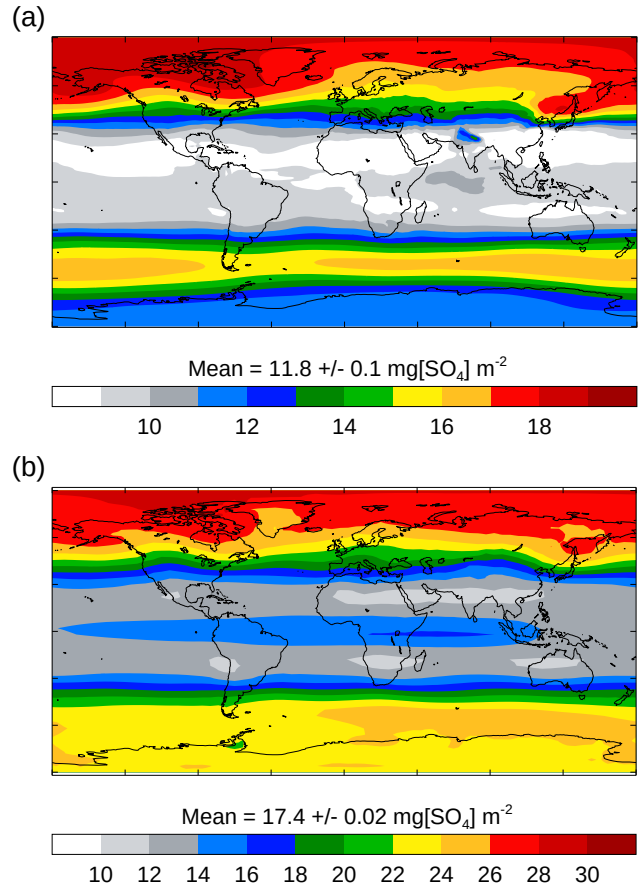

Fig. 1. Annual-mean burdens of sulphate aerosol from geoengineering (mg[SO_4] m^{-2} ± one standard deviation) for years 11–20 in **(a)** HadGEM2 and **(b)** ModelE. Distributions are calculated as the difference between the A1B and A1B-plus-geoengineering burdens in each model. Note the different scales.

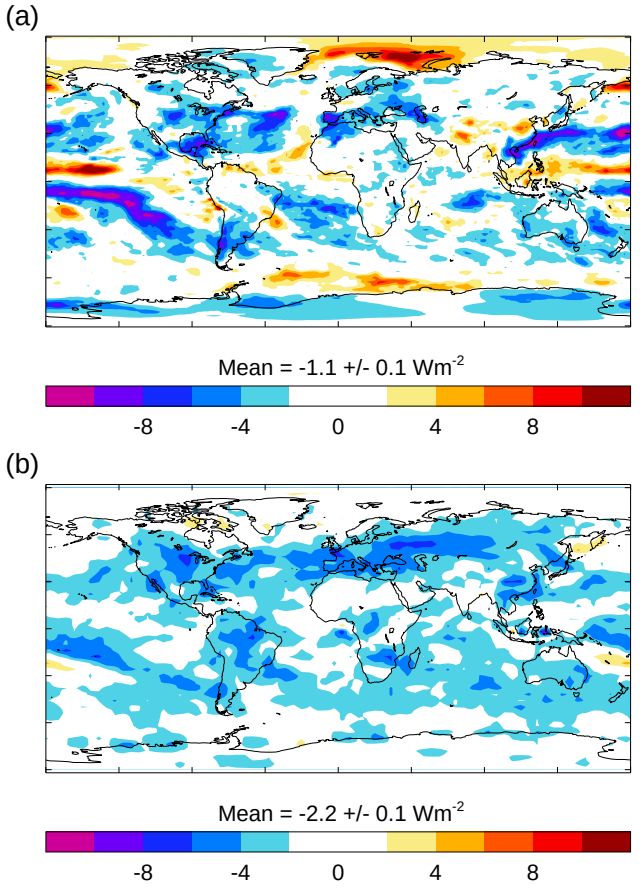

Fig. 2. Annual-mean change in incident surface shortwave radiation (W m^{-2} ± one standard deviation) due to geoengineering by SO_2 injection into the lower stratosphere averaged over the second decade in **(a)** HadGEM2 and **(b)** ModelE.

3.2 Solar radiation

Figure 2 shows the distribution of the change in downward all-sky surface shortwave radiation ($SW_\downarrow$) caused by geoengineering, averaged over the second decade for both models. The distributions are broadly similar in structure, again indicating that the difference in SO_2 injection methods is not important. The change in $SW_\downarrow$ does not follow the geoengineered aerosol burden (Fig. 1) very closely, as it also depends on the distribution of incoming solar radiation.

The global mean in ModelE is more negative than HadGEM2, consistent with the higher geoengineered aerosol burden in ModelE. The fact that there are some positive values in the distributions is because the change in $SW_\downarrow$ is the difference between parallel simulations (with and without geoengineering) which evolve with different meteorology, cloud distributions, etc. The areas of positive $SW_\downarrow$ generally correlate with areas where cloud fraction has decreased in the geoengineering simulations. The global mean changes in cloud amounts are $-0.02 \pm 0.05\%$ in HadGEM2 and $+0.25 \pm 0.03\%$ in ModelE.

A measure of the top-of-atmosphere (ToA) shortwave forcing in HadGEM2 was estimated from the difference between a further pair of simulations (with and without geoengineering), this time using an atmosphere-only configuration of the model using prescribed sea-surface temperatures and sea-ice extents to minimise surface temperature response. In ModelE, on the other hand, the ToA forcing was estimated using two calls to the radiation scheme in both the A1B and A1B-plus-geoengineering coupled simulations. In one of these calls the radiation scheme is allowed to see the sulphate aerosol, while in the other it is not. The difference between these two calls gives the forcing due to sulphate aerosol in the given simulation, and the further difference between the forcing from A1B and A1B-plus-geoengineering simulations gives an estimate of the forcing due to geoengineering sulphate. Neither the HadGEM2 nor ModelE value is a true forcing, as strictly defined, as the meteorology

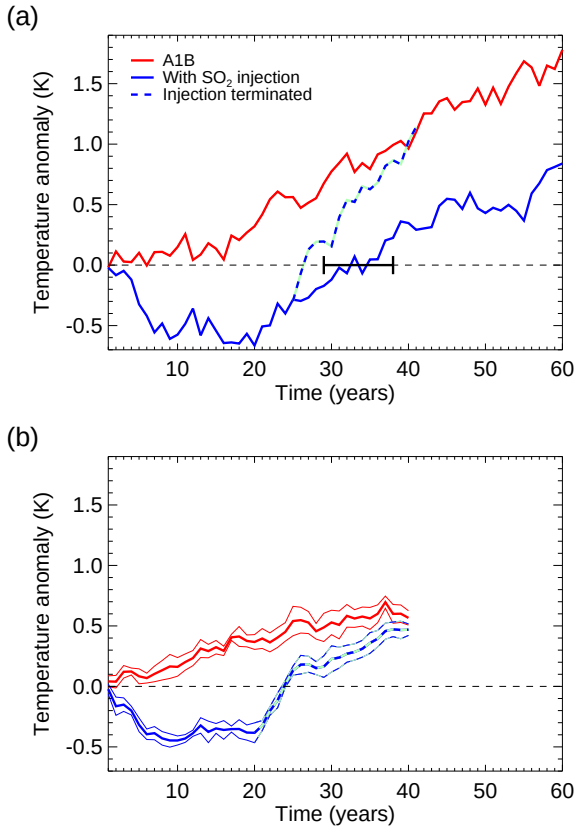

Fig. 3. **(a)** Evolution of annual global-mean near-surface air temperature anomaly (K) in HadGEM2 with respect to the 1990–1999 mean in a historical simulation. The red line is for the A1B scenario, solid blue line A1B plus geoengineering, and dashed blue line after geoengineering has been terminated. The 10-year period over which the mean near-surface air temperature anomaly is zero is marked. **(b)** As (a) but for ModelE, with the anomaly being with respect to the constant-1999 control. The thin lines indicate ±one standard deviation of the difference between the annual means of the ModelE ensemble members.

differs between HadGEM2's atmosphere-only simulations, and (obviously) between ModelE's A1B and A1B-plus-geoengineering coupled simulations. The mean ToA shortwave change is $-1.57 \pm 0.07\,\mathrm{W\,m^{-2}}$ in HadGEM2 and $-1.91 \pm 0.01\,\mathrm{W\,m^{-2}}$ in ModelE.

3.3 Surface air temperature

Figure 3 shows the evolution of global annual-mean near-surface air temperature anomaly in HadGEM2 (Fig. 3a) and ModelE (Fig. 3b). The full impact of stratospheric SO_2 injection on temperature appears to be realised in both models after about ten years of geoengineering, with mean cooling rates of -0.74 and $-0.47\,\mathrm{K\,decade^{-1}}$ in HadGEM2 and ModelE, respectively, over the first decade. This is quite a dramatic rate of temperature change, although it should be borne in mind that this is due to our idealised experimental design where geoengineering is not phased-in but is instead instantaneously fully activated.

When geoengineering is terminated the sulphate aerosol burden returns to its unperturbed state after about 5 years in HadGEM2 and global mean temperature increases at an average rate of $0.77\,\mathrm{K\,decade^{-1}}$, returning to the A1B value after about 15 years. This rate of warming is more than twice that in A1B ($0.34\,\mathrm{K\,decade^{-1}}$ over years 20–60). The behaviour of ModelE is somewhat different, warming strongly at $1.01\,\mathrm{K\,decade^{-1}}$ for the first 7 years or so, after which the rate of warming reduces to approximately $0.27\,\mathrm{K\,decade^{-1}}$ as it slowly approaches A1B temperatures. These rates compare with a mean warming of $0.16\,\mathrm{K\,decade^{-1}}$ in A1B over the whole period. The results from HadGEM2 shown in Fig. 3a suggest that a given amount of warming under the A1B scenario may be delayed by some 30–35 years by the SO_2 injection rates considered here.

Figure 4a and b shows the distribution of near-surface temperature change averaged over the second decade in HadGEM2 and ModelE, respectively. This shows cooling more or less globally in both models, with the strongest cooling at higher northern latitudes. The cooling is generally stronger over land than over ocean in both models, but HadGEM2 also shows cooling over the Arctic which is much stronger than that in ModelE. However, a problem has since been identified with the sea-ice scheme in the ModelE simulations of Robock et al. (2008) analysed here, which resulted in sea-ice being less responsive to temperature changes than it should be. This explains the differences between HadGEM2 and ModelE at high latitudes, and also contributes to the lower climate sensitivity of ModelE compared with HadGEM2. This also suggests that the similarity of global-mean temperature change in the two models ($-0.74\,\mathrm{K}$ in HadGEM2 and $-0.69\,\mathrm{K}$ in ModelE in the second decade) is coincidental.

However, the important point is that, with the exception of extreme northern latitudes, the distribution of temperature response in the two models is in reasonable agreement, with HadGEM2 showing a more detailed geographic pattern due to the higher resolution of the model and the fact that it is a single model experiment rather than a small ensemble.

One definition of the goal of geoengineering could be to avoid any further global warming due to continuing increases in GHG concentrations. Figure 3a shows that after about 30 years of the geoengineering simulation the global-mean near-surface air temperature in HadGEM2 is about the same as at the start of the simulation, i.e. the same as the mean 1990–1999 period. It is therefore instructive to examine the mean changes for the 10-year period over which the mean temperature anomaly is approximately zero (mean of years 29–38 inclusive), which period one could consider as being an analogue for geoengineering counterbalancing global warming. The changes in temperature are shown in Fig. 4c for HadGEM2. Although the global-mean temperature change

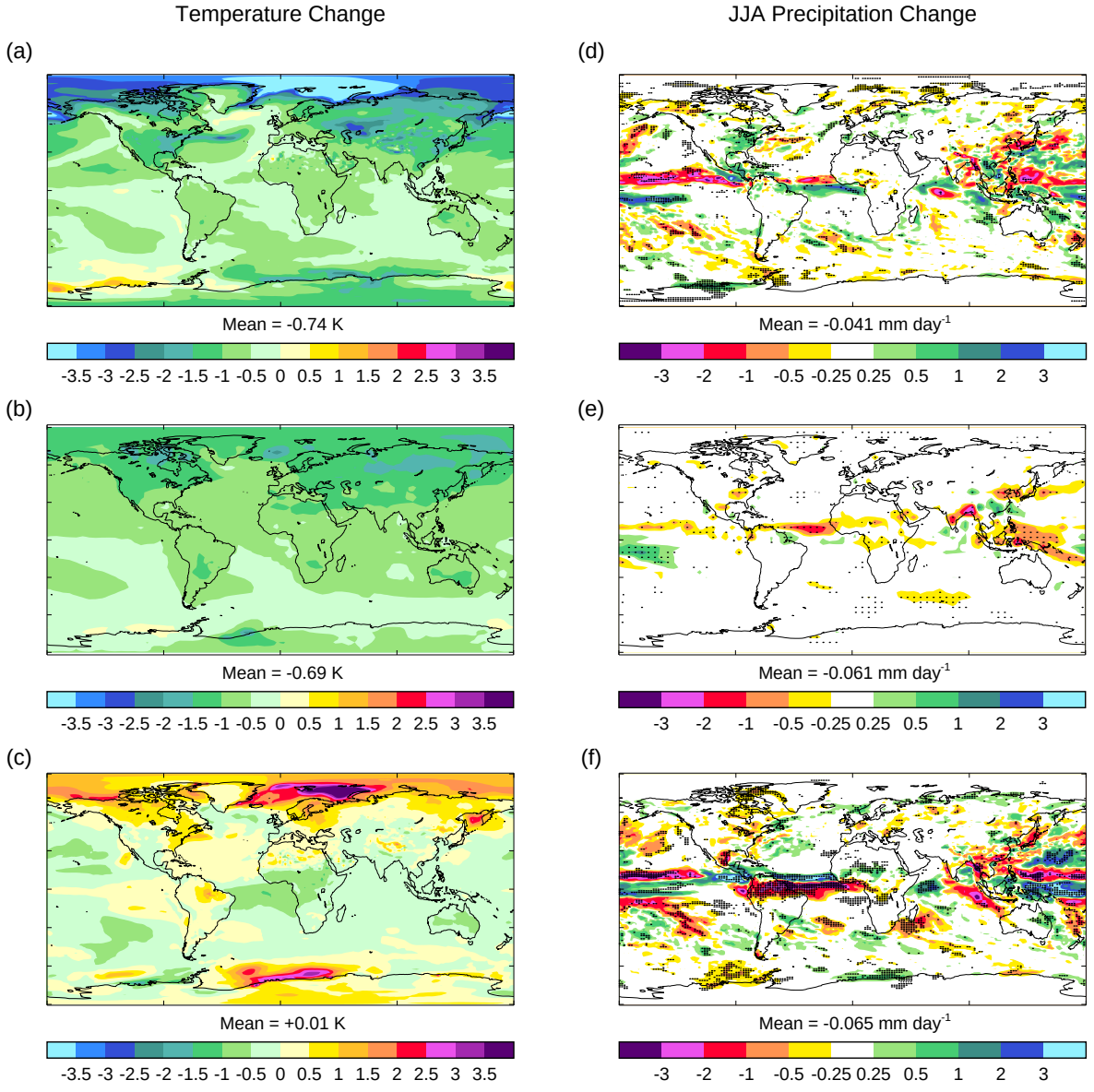

Fig. 4. **(a)** Difference in annual-mean near-surface air temperature (K) between the A1B-plus-geoengineering and A1B simulations in HadGEM2, meaned over the second decade of simulation. **(b)** As (a) but for ModelE. **(c)** As (a) but comparing years 29–38 of the A1B-plus-geoengineering simulation with the 1990–1999 period in a historical simulation. **(d)** As (a) but for change in mean June-August precipitation rate (mm day^{-1}) in HadGEM2; areas where changes are significant at the 5% level are indicated by dots. **(e)** As (d) but for ModelE. **(f)** As (c) but for change in mean June–August precipitation rate.

may be near zero (+0.01 K), regionally this is far from the case. Some land areas such as central Africa and Australia are cooler than the 1990–1999 mean by up to 1 K, whereas the Amazon region is warmer by a similar amount. Polar amplification due to ice-albedo feedbacks are also apparent in the warming at high latitudes, indicating that the cooling effect of geoengineering at these latitudes (Fig. 4a) has by this time been overwhelmed by the warming due to GHGs.

3.4 Precipitation

The mean change in June–August precipitation rate is shown in Fig. 4d and e for HadGEM2 and ModelE, respectively. While the distributions clearly differ in some areas (e.g. ModelE shows a reduction of precipitation in the eastern USA, whereas HadGEM2 suggests an increase), nevertheless the results from both models again share certain broad features. Tropical precipitation maxima over the Atlantic and

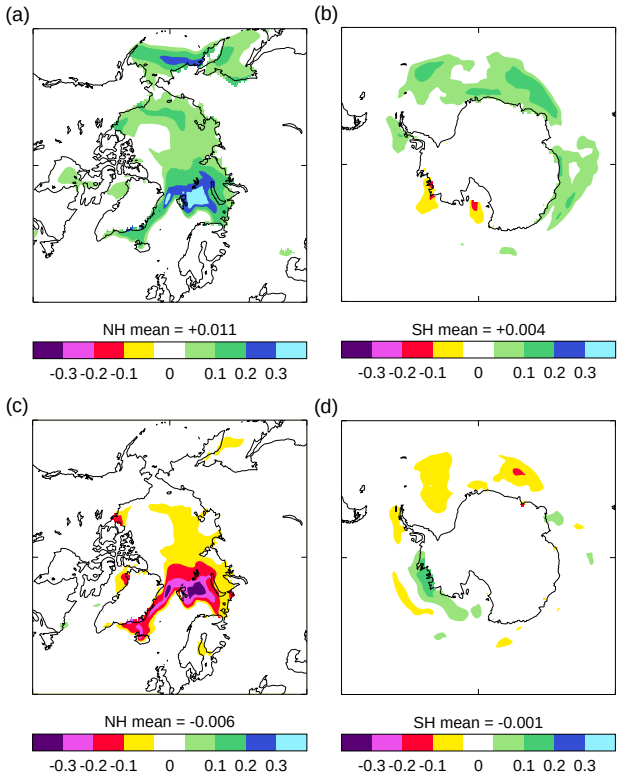

Fig. 5. Difference in HadGEM2 decadal-mean hemispheric sea-ice fractions between: **(a)** and **(b)** the A1B-plus-geoengineering and A1B simulations meaned over the second decade of simulation, and **(c)** and **(d)** the second decade of A1B and the 1990–1999 period in the historical simulation.

much of the Pacific oceans are displaced southwards in both models, resulting in precipitation reductions in sub-Saharan Africa and the land areas around the Bay of Bengal. This is in response to the hemispheric asymmetry in the temperature change (Fig. 4a), such that the precipitation maximum associated with the inter-tropical convergence zone (ITCZ) moves southwards towards the warmer hemisphere (e.g., Williams et al., 2001; Rotstayn and Lohmann, 2002).

It must be remembered that the changes in precipitation described above are with respect to the corresponding period (years 11–20) of the A1B simulations, not with respect to approximately current conditions. Further, the geoengineering simulations during this period are considerably cooler than current conditions due to the idealised manner in which SO_2 injection is applied. The change in mean June-August precipitation in HadGEM2 between the 1990–1999 mean and the years 29–38, the decade when global-mean temperature is about the same as the 1990–1999 period, is shown in Fig. 4f. As well as a reduction in global-mean precipitation, consistent with the results of Bala et al. (2008) and Robock et al. (2008), there are also significant changes in regional precipitation, despite the fact that employing geoengineering has meant virtually no change in global-mean temperature. The precipitation maximum associated with the ITCZ has generally moved northwards in response to the asymmetric warming, and although geoengineering has somewhat ameliorated this change (as shown in Fig. 4d, indicating the tendency of the geoengineering to move the ITCZ southwards), the changes induced by increasing GHG concentrations clearly dominate.

3.5 Sea-ice

We only show the sea-ice changes from HadGEM2 due to the problems with the sea-ice scheme in the ModelE results noted above. Comparing the second decade from the geoengineering simulation with the corresponding A1B simulation, Arctic sea-ice area increased by 2.71×10^6 km^2, and Antarctic sea-ice area by 0.92×10^6 km^2, as shown in Fig. 5. This compares with decreases of 1.61 and 0.27×10^6 km^2 for Arctic and Antarctic sea-ice area, respectively, when comparing the second decade of A1B with the mean of 1990–1999 in the historical simulation. The larger change in Fig. 5a and b compared with 5c and d is directly related to the temperature differences between the two simulations in their second decade compared with that in the 1990–1999 control (Fig. 3a).

4 Discussion and conclusions

We have compared the impact of geoengineering by stratospheric SO_2 injection in two fully coupled climate models, HadGEM2 and ModelE. These models differ in numerous ways, having different resolutions, using different SO_2 injection methods, and producing different magnitudes of geoengineered sulphate aerosol burdens. Despite these differences, however, injecting the same amount of SO_2 into the lower stratosphere induces climate responses which show considerable agreement between the two models. Both suggest a reduction in near-surface air temperature which is global in extent and distributed in a similar fashion to the warming caused by GHGs (e.g. Fig. 6a in Jones et al., 2009). Both models also indicate that this form of geoengineering causes a southward displacement of the tropical precipitation maximum. This may counteract to some degree the northward shift caused by increases in GHG concentrations, but the latter still dominate.

The HadGEM2 simulations suggest that the SO_2 injection rates considered here could defer a given amount of global-mean warming under the A1B scenario by 30–35 years. However, both models also indicate a rapid warming if geoengineering is not maintained, which raises serious issues when considering the amount of time over which geoengineering would need to be sustained.

The patterns of temperature and precipitation responses to geoengineering via stratospheric SO_2 injection differ from

those via modification of marine stratocumulus cloud sheets in HadGEM2 (Jones et al., 2009). The stratospheric SO_2 injection geoengineering simulations produce geographic responses which, being more homogeneous, more closely counteract the responses due to increasing concentrations of GHGs than do the responses from stratocumulus modification. However, the results from HadGEM2 suggest that increases in GHG concentrations can still have a profound impact on regional climate even if geoengineering is successful in counteracting any change in global-mean temperature. Maintaining global-mean temperature near its current level might be considered a necessary goal for any geoengineering proposals, but it is by no means sufficient. It should also be borne in mind that, in common with other geoengineering proposals to modify the Earth's radiation balance, stratospheric SO_2 injection does nothing to offset other impacts of increasing GHG concentrations, such as ocean acidification. Furthermore, neither model addresses the potential damage to the ozone layer caused by deliberate introduction of stratospheric aerosols (e.g. Crutzen, 2006).

The similarity of the temperature and precipitation responses in the two models hardly constitutes a consensus on the impacts of geoengineering via stratospheric SO_2 injection across the scientific community. It is therefore important for many different climate models to assess the impact of such geoengineering, ideally using a common experimental design as suggested for GeoMIP (Kravitz et al., 2010). This should be done before any consideration is given to practical implementation of such proposals.

Acknowledgements. We would like to thank Luke Oman for performing the ModelE simulations and providing helpful information, and Georgiy Stenchikov for useful comments. The work of BK and AR was supported by National Science Foundation grant ATM-0730452. Model development and computer time at Goddard Institute for Space Studies are supported by National Aeronautics and Space Administration climate modeling grants. AJ, JH and OB were supported by the UK Joint DECC and Defra Integrated Climate Programme – DECC/Defra (GA01101).

Edited by: A. Baumgaertner

References

d'Almeida, G. A., Koepke, P., and Shettle, E. P.: Atmospheric aerosols: global climatology and radiative characteristics, A. Deepak Publishing, Hampton, USA, 1991.

Bala, G., Duffy, P. B., and Taylor, K. E.: Impact of geoengineering schemes on the global hydrological cycle, Proc. Nat. Acad. Sci., 105, 7664–7669, doi:10.1073/pnas.0711648105, 2008.

Bellouin, N., Boucher, 0., Haywood, J. M., Johnson, C. E., Jones, A., Rae, J.G.L., and Woodward, S.: Improved representation of aerosols for HadGEM2, Hadley. Cent. Tech. Note 73, Met Office, Exeter, UK, available at: http://www.metoffice.gov.uk/publications/HCTN/index.html, 2007.

Collins, W. J., Bellouin, N., Doutriaux-Boucher, M., et al.: Evaluation of the HadGEM2 model, Hadley. Cent. Tech. Note 74, Met Office, Exeter, UK, available at: http://www.metoffice.gov.uk/publications/HCTN/index.html, 2008.

Crutzen, P.: Albedo enhancement by stratospheric sulfur injections: A contribution to resolve a policy dilemma?, Clim. Change, 77, 211–220, doi:10.1007/s10584-006-9101-y, 2006.

Haywood, J. M. and Schulz, M.: The reduction of uncertainty in estimates of the anthropogenic radiative forcing of climate between IPCC (2001) and IPCC (2007), Geophys. Res. Lett., 34, L20701, doi:10.1029/2007GL030749, 2007.

IPCC: Climate Change 2001: The Scientific Basis. Contribution of Working Group I to the Third Assessment Report of the Intergovernmental Panel on Climate Change, edited by: Houghton, J. T., Ding, Y., Griggs, D. J., et al., Cambridge University Press, Cambridge, UK and New York, USA, 2001.

IPCC: Climate Change 2007: The Physical Science Basis. Contribution of Working Group I to the Fourth Assessment Report of the Intergovernmental Panel on Climate Change, edited by: Solomon, S., Qin, D., Manning, M., et al., Cambridge University Press, Cambridge, UK and New York, USA, 2007.

Jones, A., Roberts, D. L., Woodage, M. J., and Johnson, C. E.: Indirect sulphate aerosol forcing in a climate model with an interactive sulphur cycle, J. Geophys. Res., 106, 20293–20310, doi:10.1029/2000JD000089, 2001.

Jones, A., Haywood, J., and Boucher, O.: Climate impacts of geoengineering marine stratocumulus clouds, J. Geophys. Res., 114, D10106, doi:10.1029/2008JD011450, 2009.

Koch, D., Schmidt, G. A., and Field, C. V.: Sulfur, sea salt, and radionuclide aerosols in GISS ModelE, J. Geophys. Res., 111, D06206, doi:10.1029/2004JD005550, 2006.

Kravitz, B., Robock, A., Stenchikov, G., Taylor, K., Boucher, O., Schmidt, H., and Schulz, M.: The Geoengineering Model Intercomparison Project (GeoMIP), Atmos. Sci. Lett., submitted, 2010.

Nakićenović, N., , Alcamo, J., Davis, G., et al.: IPCC Special Report on Emission Scenarios, Cambridge Univ. Press, Cambridge, UK, 2000.

Rasch, P. J., Tilmes, S., Turco, R. P., Robock, A., Oman, L., Chen, C.-C., Stenchikov, G. L., and Garcia, R. R.: An overview of geoengineering of climate using stratospheric sulphate aerosols. Philos. Trans. R. Soc. A, 366, 4007–4037, doi:10.1098/rsta.2008.0131, 2008.

Robock, A.: Volcanic eruptions and climate, Revs. Geophys., 38, 191–219, 2000.

Robock, A., Oman, L., and Stenchikov, G. L.: Regional climate responses to geoengineering with tropical and Arctic SO_2 injection, J. Geophys. Res., 113, D16101, doi:10.1029/2008JD010050, 2008.

Rosenlof, K. H.: Seasonal cycle of the residual mean meridional circulation in the stratosphere, J. Geophys. Res., 100, 5173–5191, 2008.

Rotstayn, L. D. and Lohmann, U.: Tropical rainfall trends and the indirect aerosol effect, J. Climate, 15, 2103–2116, 2002.

Russell, G. L., Miller, J. R., and Rind, D.: A coupled atmosphere-ocean model for transient climate change, Atmos. Ocean, 33, 683–730, 1995.

Schmidt, G. A., Ruedy, R., Hansen, J. E., et al.: Present day atmospheric simulations using GISS ModelE: Comparison to in-situ, satellite and reanalysis data, J. Climate, 19, 153–192, doi:10.1175/JCLI3612.1, 2006.

Tang, I. N.: Chemical and size effects of hygroscopic aerosols on light scattering coefficients, J. Geophys. Res., 101(D14), 19245–19250, 1996.

Williams, K. D., Jones, A., Roberts, D. L., Senior, C. A., and Woodage, M. J.: The response of the climate system to the indirect effects of anthropogenic sulfate aerosols, Clim. Dynam., 17, 845–856, 2001.